Automated Measurement of Liquid-liquid Equilibria using Raman Spectroscopy and Single Droplet Tracking in Microfluidic Plug Flow

Fluid Phase Equilibria 567 (2023) 113718

Contents lists available at ScienceDirect

Fluid Phase Equilibria

journal homepage: www.journals.elsevier.com/fluid-phase-equilibria

Automated Measurement of Liquid-liquid Equilibria using Raman Spectroscopy and Single Droplet Tracking in Microfluidic Plug Flow

Marvin Kasterke [‡,a], Julia Thien [‡,a], Carsten Flake [a,b], Thorsten Brands [a], Leo Bahr [a], André Bardow [a,b], Hans-Jürgen Koß [a,*]

[a] Institute of Technical Thermodynamics, RWTH Aachen University, 52062 Aachen, Germany
[b] Energy & Process Systems Engineering, ETH Zürich, 8092 Zürich, Switzerland

ARTICLE INFO

Keywords:
Liquid-liquid equilibrium
Microfluidics
Plug flow
Raman Spectroscopy
Automation

ABSTRACT

Raman spectroscopy has proven to be a powerful tool for the highly efficient and automated determination of liquid-liquid equilibria (LLE) in parallel microfluidic flows. However, a stable parallel microfluidic flow regime cannot be established for numerous industrially relevant aqueous-organic LLE systems since they tend to form plug flows. These plug flows have the advantage that inner circulations in the plugs enhance the mass transfer, leading to a much faster equilibration. For moving plugs, the main challenge is that established techniques are not capable to collect sufficient Raman signal for quantification. Therefore, we developed a measurement setup for LLE in microfluidic plug flows. In our setup, a capillary is moved against the flow direction to hold one plug of either the aqueous or the organic phase in the laser focus during the Raman measurement. Full automation is established for the premixing of the components, the calculation of the plug lengths and speeds and the Raman measurements of both phases. The setup and automated measurement procedure are successfully validated by showing excellent agreement with data from the literature for the LLE of the ternary system acetone – toluene – water at $t = 25$ °C. The developed setup thus enables efficient access to LLE data for industrially relevant mixtures.

1. Introduction

Reliable experimental data for liquid-liquid equilibria (LLE) remain the basis of accurate extraction column design in the chemical industry [1]. The optimal design and operation of extraction columns requires not only distribution coefficients, but also the concentration-dependent mutual solubility between the feed and solvent phase and, thus, the full LLE data. Since conventional experiments are time- and material-consuming [2], experimental LLE data is scarce, in particular for multicomponent systems [1]. Additionally, screenings of new systems are often limited by the availability of the components. Therefore, fast LLE experiments are needed that require only small samples.

Recent approaches for more efficient LLE experiments achieved smaller sample volumes and automation by combining an autosampler with standard analytical methods like gas chromatography (GC) or high performance liquid chromatography (HPLC) [3,4]. These analytical techniques need long analysis times and are therefore rate-limiting. Alternative approaches conduct high throughput in-situ measurements of LLE in small glass tubes using nuclear magnetic resonance spectroscopy (NMR) [5]. However, the availability of NMR equipment is quite limited. Hübner and Minerva [6] recently presented a microfluidic setup for the determination of LLE without any composition determination by an analytical device. In their setup, the LLE concentrations were calculated under knowledge of the position of the binodal curve from the measured densities of both saturated phases and the position of the phase boundary. The approach of Hübner and Minerva uses the assumption that the two liquid phases flow side by side at the same velocity, which is only valid if the ratios of the viscosities and densities are close to one [6]. Furthermore, especially for the screening of new systems, the position of the binodal curve is often not known.

We recently presented an automated microfluidic platform for highly efficient calibration and determination of LLE data using Raman microspectroscopy [7]. The small dimensions of the microchannel enable small sample volumes and rapid equilibration. The equilibrated

* Corresponding author.
E-mail address: hans-juergen.koss@ltt.rwth-aachen.de (H.-J. Koß).
‡ M. Kasterke and J.Thien contributed equally to this work.

https://doi.org/10.1016/j.fluid.2022.113718
Received 23 November 2022; Received in revised form 21 December 2022; Accepted 27 December 2022
Available online 29 December 2022

compositions are analyzed rapidly using in-situ Raman microspectroscopy. The automation of the setup avoids manual sample preparation substantially reducing the experimental effort and enabling user-independent experimental results. The previously presented microfluidic platform contacted two immiscible liquid flows at a small angle at the entry of an H-cell microchannel to form a laminar flow regime. Due to the steady-state flow, phase-specific Raman spectra can easily be acquired at fixed positions along the channel length. However, the laminar flow limits the mass transfer to diffusion only. As a result of the low diffusive mass transfer rates, the equilibrium cannot always be reached within the length of the microchannel. These low mass transfer rates are particularly an issue for the industrial relevant water-organic LLE systems. Furthermore, laminar flows are hard to establish in long microchannels due to the rising Kelvin-Helmholtz (KH) instability in consequence of velocity difference across the phase boundary and pressure imbalance [8]. In their review of microfluidic liquid-liquid extractors Xu and Xie therefore found that all laminar flow microextractors without membranes are shorter than 7 cm [8]. This constraint limits the application domain of laminar flow contactors for LLE measurements.

As an alternative, plug flows can be established by contacting two immiscible liquid flows in a junction at relatively low and similar flow rates, where interfacial forces dominate. These plug flows have the advantage that the equilibration is much faster than in parallel flows: larger surface-to-volume ratios and convective circulation within the plugs increase the interfacial mass transfer by orders of magnitude [9]. The great potential of microfluidic plug flows for liquid-liquid extraction has been shown: the extraction efficiency is enhanced strongly compared to parallel microfluidic flows [10,11].

Microfluidic plug flows have also already been successfully employed to determine distribution coefficients. Thereby, the concentrations were determined either by using offline standard analytics after phase separation [12–15] or using in-situ analytics like epifluorescence microscopy [16,17] and Raman spectroscopy [18,19].

However, to the best of our knowledge, no full LLE measurements have been conducted in microfluidic plug flows until now. The main challenge for using in-situ analytics in combination with plug flows is that mechanisms are needed for phase-selective data acquisition in the moving plugs. This requirement is particularly difficult to satisfy since the phase distribution and, consequently, the plug lengths are not predictable for unknown LLE systems. Taking snapshots of individual moving plugs is possible when using epifluorescence spectroscopy, which allows for high signal intensities. However, only one single fluorescent component can be determined, allowing only determining its concentration and thus the distribution coefficient [16,17]. In contrast, Raman spectroscopy can distinguish between a wide range of molecules [20]. Nevertheless, a Raman signal from a single plug crossing a fixed measurement volume is often too weak for a precise quantitative analysis. For this reason, Luther *et al.* accumulate the Raman signal from numerous plugs using a photo-electric guard [21]. Their setup thus requires averaging spectra of multiple plugs and does not allow to investigate one single plug.

In addition to the challenge of recording phase-selective spectra, there is also the challenge of quantitatively evaluating these spectra. Since Raman signals of liquid components are strongly overlapping, accurate methods are required for spectra evaluation when small concentrations need to be quantified precisely. Especially, the water signal analysis is quite challenging for low water concentrations in organic phases since the Raman signal of water is very weak and it additionally changes its shape significantly due to disappearing hydrogen bonds [22].

Here, we present a setup for full LLE determination based on automated droplet detection and tracking in combination with phase-selective Raman spectroscopy measurements in single plugs of a microfluidic plug flow. A low-cost camera and a traversing unit enable the phase-selective data acquisition of single plugs. The camera detects plugs flowing inside a capillary. Through image processing, the velocities and sizes of the plugs are estimated from the recordings of the camera. Once a stable flow regime is reached, the traversing unit moves the capillary with the plug velocity opposite to the flow direction to keep a single equilibrated plug stationary in the focus of the optical measurement setup. The novel setup is demonstrated for the ternary system acetone – toluene – water and the results are compared to literature.

2. Automated experimental setup and workflow

The experimental setup consists of a syringe pump unit, a micromixer, a capillary which includes a droplet detection unit (DDU) and is installed on a traversing unit, a laser and a spectrometer (Fig. 1).

Pure components are dosed via three independent syringe pumps (Mid-Pressure Syringe Pump neMESYS, Cetoni GmbH, Germany). The global concentration can be varied by adjustment of the volume flow ratios so that the time-consuming and error-prone manual sample preparation is omitted, and the complete phase diagram is accessible in a single experiment [7]. For the conducted LLE experiments, acetone and toluene are premixed in the micromixer (Swirl Micromixer, Micronit, The Netherlands) and contacted with water in a T-junction (PEEK Tee, CS-Chromatographie Service GmbH, Germany). The T-junction is used for droplet generation at the beginning of the capillary, to form a stable liquid-liquid plug flow [23]. To connect the syringe pumps to the micromixer and capillary, PTFE tubing with an inner diameter of 300 μm and connection parts from PEEK are used. The used capillary is made of fused silica and has an inner diameter of 530 μm and a length of 45 cm. The end of the capillary is open and the liquid flowing out is collected. A traversing unit (isel-automation, Germany) can move the capillary against the flow direction to hold the laser focus in the center of one plug. The maximum distance that the traversing unit can pass has shown to be 15 cm. Thereby, the biggest challenge is to install the capillary straight enough to keep the focus in the center of the capillary.

Due to the wetting characteristics of the glass capillary, the aqueous phase is the continuous phase, and the organic phase is the dispersed phase in the established plug flow. The plugs of the organic phase are therefore surrounded by a very thin film of the aqueous phase which wets the wall completely. The mass transfer is enhanced due to inner circulations and the resulting homogenous concentrations inside the plugs that keep the concentration gradient high for diffusion across the phase boundary [10].

A droplet detection unit is installed at a distance of 300 mm from the capillary entry (Fig. 2). A camera (Logitech C270) is directed at the capillary and continuously provides pictures of the plug flow. Four white LEDs next to the camera illuminate the capillary (Fig. 2a). The complete system is encapsulated so that the light of the LEDs does not impair the Raman measurements. The cameras images are read out and processed by National Instruments LabVIEW 2019 to determine the droplet speeds and lengths. Two brightness control lines are set in the camera image as ranges of interest (ROI) at a fixed distance s to each other in flow direction (Fig. 2b). These brightness control lines are placed near the glass surface of the capillary since the phases can best be distinguished here due to the different wetting characteristics of the two phases with the glass wall and the resulting shadow between the plugs of the organic phase and the glass surface (Fig. 2b). The intensity values of the pixels of the two ROI lines were read out continuously and the Labview Script thus detects the change in the light intensity when a Shadow of a phase boundary passes a ROI line. The velocity of the plug flow v is calculated from the time Δt that the plugs need to overcome the distance s. This time delay Δt is calculated from the delay between the edges of the data patterns of ROI 1 and ROI 2 (respectively rising or falling, s. Fig. 2c).

For the acquisition of the Raman spectra, a confocal setup is used which records the Raman scattered light in backscattering (Fig. 1). A laser beam of a 532 nm Nd:YAG laser (Genesis CX532–2000 SLM, COHERENT, 150 mW) is focused through a lens (N-BK7 Plano-Convex Lens, f = 30 mm, A Coated, Thorlabs) onto the sample in the

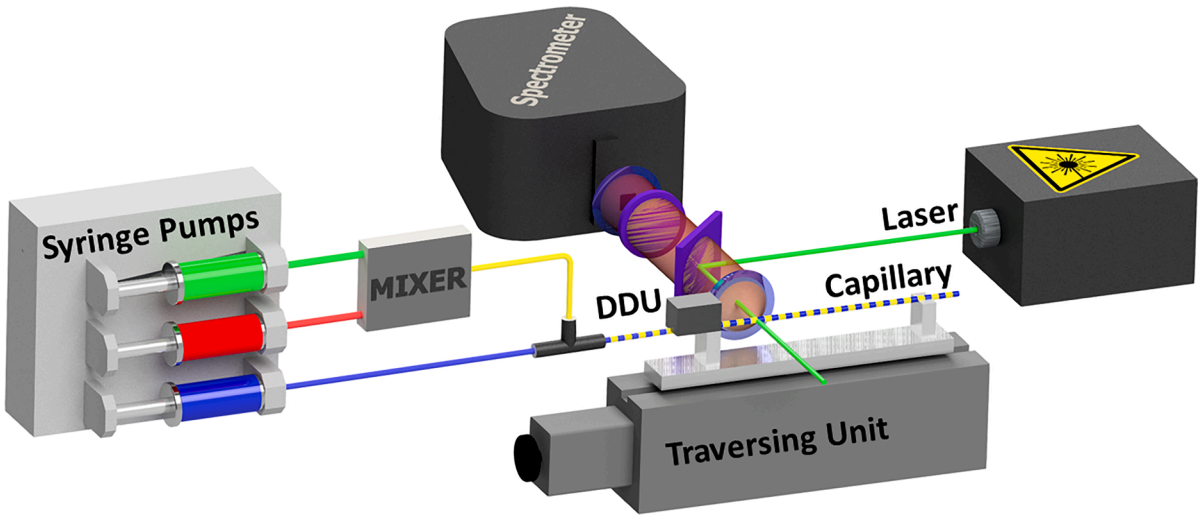

Fig. 1. Experimental Setup with syringe pumps, micromixer, traversing unit, droplet detection unit (DDU), capillary, laser, and spectrometer.

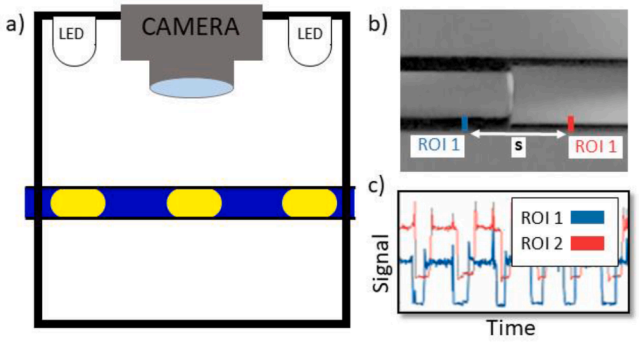

Fig. 2. Droplet detection unit (DDU): a) Camera captures images of the illuminated capillary. b) Camera image with two defined ranges of interest (ROI) at a fixed distance *s* to each other. c) Signal over time at ROI 1 and ROI 2.

measurement volume inside the capillary. Due to the focusing of the laser, an influence of the small film of the aqueous phase on the spectrum of the organic phase can be excluded. The backscattered Raman light is separated from the laser light by two dichroic filter (Raman Strahlenteiler RT 532 rdc, AHF Germany, dividing line a 532 nm, 45 °; Semrock 532 nm StopLine single-notch filter, 0 °) and focused on the slit of a spectrometer (IsoPlane SCT320, Princeton Instruments). The spectrally resolved Raman light is recorded by a CCD sensor of a camera (ProEM 16,00^4, Princeton Instruments) and saved by the Princeton Instruments Lightfield 5.0 software.

The traversing unit, holding T-Junction and droplet detection unit, is encapsulated from the laboratory environment by a 54.5 × 35 × 30 cm^3 temperature-controlled polystyrene box. This box is omitted for clarity in Fig. 1. A heat exchange system is installed inside the box to control and ensure temperature stability. A Haake Phoenix II P50C thermostat with an external Pt100 sensor, combined with a heat exchanger (MagiCool, G2 Slim Radiator 16 FPI – 240 mm), regulates the temperature to $t = 25 \pm 0.2$ °C. To ensure fast heat transfer and homogeneous temperature distribution, the heat exchanger is ventilated by two 120 mm fans (Arctic P12PWM PST).

A new mixture is analyzed by first recording calibration spectra from weighed-in samples which are injected into the capillary. In this work, for each calibration point, 100 spectra were recorded with an exposure time of 300 ms. The calibration samples must be located in the homogeneous region outside the miscibility gap of the LLE system. Here, for the proof of concept, the location of the miscibility gap is known from literature. For a completely unknown system, the location of the miscibility gap can be estimated by a predictive thermodynamic model like COSMO-RS [24].

For the LLE experiments, several global concentrations were chosen inside the miscibility gap. Fig. 3 shows the scheme of the automated workflow to measure one equilibrium point. To start an experiment, a graphical user interface of the program allows to set the experimental parameters (number of experiments and for each experiment volume flow rates of individual components and number and exposure time of Raman acquisitions). After the initialization of the syringe pumps, the system waits 10 min which, in preliminary tests, has proven to be a typical time between the adjustment of the volume flow rates at the syringe pumps and establishing the set composition and a stable plug flow in the capillary. This so-called start-up period depends on the length of the connection parts. After this start-up period, the labview script automatically determines the droplet lengths and speeds from the camera pictures of the droplet detection unit. For this, the system-specific threshold values for the distinction between the phases are automatically determined from evaluating the intensity values of the ROI lines over multiple alternating droplets. This procedure is performed separately for each ROI-line because the illumination of the capillary is not homogeneous, and the ROI-lines are located at different positions. The system checks for steady state by calculating the deviation of the measured droplet velocities with the theoretical velocities from the volume balance of the dosing. If the deviation is within a range of 1.45 mm/s, steady state is assumed. After reaching the steady state, the system tracks the next passing plug, and the spectrometer starts acquiring spectra with the specified exposure time and number of spectra. Here, 25 spectra with an exposure time of 300 ms are recorded in each plug. At the end of the measurement, the traversing unit returns to the initial starting position and a plug of the other phase can be tracked.

Afterwards, the volume flow rates are adjusted to the next global concentration and the automated procedure from Fig. 3 is repeated.

To validate the setup, the LLE of the ternary system acetone – toluene – water is measured. The measured mole fractions are compared to literature data from Friebel et al. at $t = 22$ °C [5]. All chemicals are used as received. Suppliers, specifications, and purities of the used chemicals are listed in table 1.

3. Data analysis

The Raman spectra are evaluated quantitatively using the Indirect Hard Modeling (IHM) approach [25,26] implemented in the PEAXACT 4

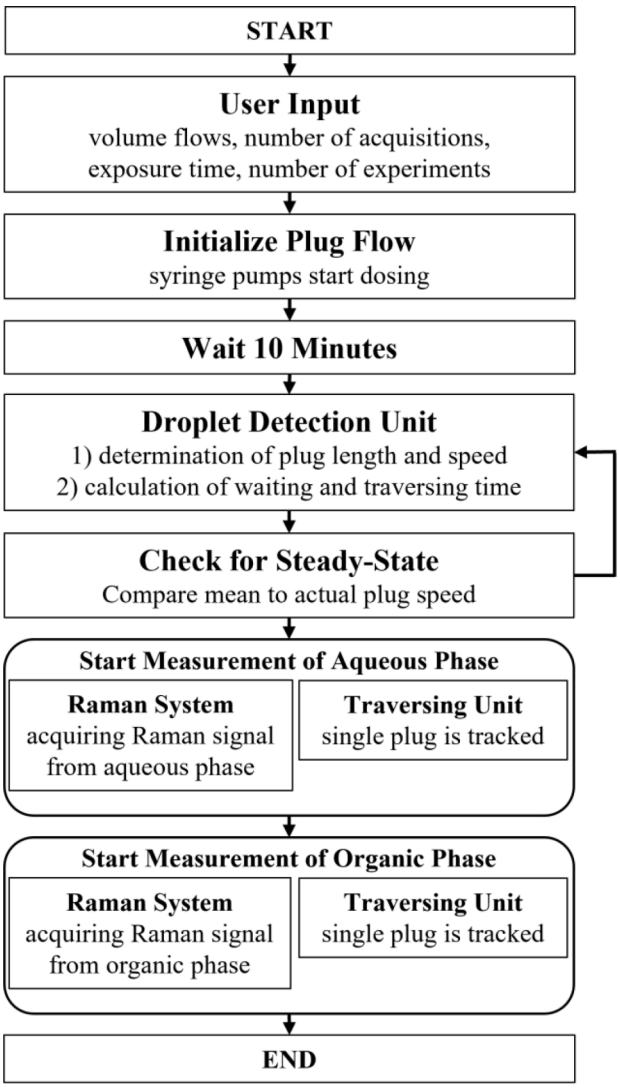

Fig. 3. Scheme of the automated experimental procedure for liquid-liquid equilibrium measurements.

Table 1
Used chemicals with supplier, specification, and purity in gas-chromatography area percentage (GC, A%) from supplier data.

	CAS number	supplier	description	purity (GC, A %)
acetone	67–64–1	VWR	Spectronorm	99.9
toluene (ethyl benzene)	108–88–3	VWR	Spectronorm	99.8
water	7732–18–5	VWR	Spectronorm	99.9

software (S-PACT GmbH, Germany). IHM has proven to be very suitable for quantifying liquid multicomponent mixtures with strongly overlapping spectral bands [27]. A detailed description of the method can be found in our previous work [7]. The IHM method models pure component spectra by a sum of pseudo-Voigt functions. The resulting pure component models build up a linear mixture model which is fitted to a mixture spectrum, while nonlinear mixture effects as peak shifts are considered by the release of related peak parameters of the pseudo-voigt functions. The fit gives the weights w_i of each pure component i in the mixture spectrum. These weights w_i are proportional to the corresponding mole fractions of component i in the mixture so that a linear calibration model can be used for the calculation of the mole fractions x_i:

$$\frac{w_i}{w_j} = k_{ij}\frac{x_i}{x_j} \; for \; i = 1, \; \ldots, \; n \tag{2}$$

$$\sum_{i=1}^{n} x_i = 1. \tag{3}$$

The calibration constants k_{ij} are determined from the known calibration spectra. Here, we chose two different calibration sets according to the expected concentration ranges of the two phases. Water's specific spectral behavior requires these two calibration sets for high accuracy: The shape of liquid water's Raman spectrum depends on the degree of hydrogen bonding and is thus not constant. With progressing dilution, the hydrogen bonds, whose vibrations make up a large part of the pure component Raman spectrum of water, disappear. Thus, the intensity of the water peak is not proportional to the concentration over the complete concentration range, as it is normally the case for other components. Additionally, the Raman spectrum of diluted water is completely different to the Raman spectrum of pure water (Fig. 4). Therefore, the pure component spectrum of water can only be used to build the pure component model of water in the aqueous phase. In the organic phase however, the water concentration is low, and the hydrogen bonds vanish so that a single peak builds the pure component model of water (Fig. 5) [28]. The pure component models of acetone and toluene, which are built from the respective pure component spectra, can be used for both calibration sets (figures S1 and S2 in the SI).

For the industrially relevant water-organic LLE systems, quantifying water as an analyte is especially challenging at the low concentrations in the organic phase. Compared to organic compounds, water shows a weak Raman cross-section, especially at lower wavenumbers. To increase the relative area of water in the mixture spectrum, the analysis of the organic phase only employs the part with relative wavenumbers $>$ 2500 cm^{-1} for the spectral evaluation.

The calibration data is presented in the SI, including the weighed-in mole fractions and a comparison between measured and set mole fractions for all components in both water-rich and toluene-rich calibration area.

In the LLE experiments, absolute standard uncertainties are obtained from arithmetic averaging over 25 spectra recorded with an exposure time of 300 ms for each spectrum during single plug tracking. These uncertainties thus represent the measurement variance. The set volume flow rates of the conducted LLE experiments are presented in table S3 in the SI.

4. Results and discussion

With the introduced automated setup, nine different LLE

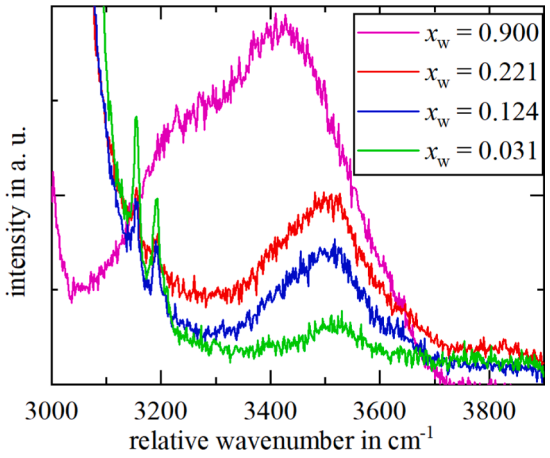

Fig. 4. OH-stretching vibration band of the Raman spectrum of water changes shape and position with increasing dilution.

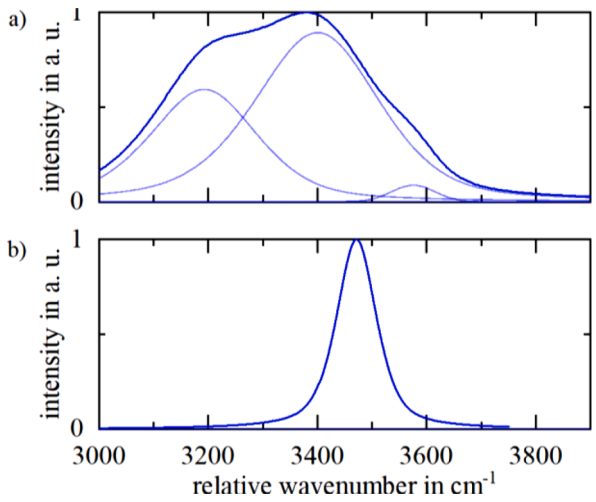

Fig. 5. IHM pure component models of water: a) IHM model of water in aqueous phase consisting of three peaks. b) IHM model of water in organic phase consisting of one single peak.

compositions of the ternary system water – acetone – toluene were successfully determined. For each equilibrium composition, a single plug of either organic or aqueous phase has been tracked and measured successfully. Single droplet tracking provides the additional advantage of checking if the equilibrium is reached. Fig. 6 and figures S9 to S16 in the SI show the development of the mole fractions in on single plug of either aqueous or organic phase during the tracking time of about 10 s. All measured mole fractions in all single plugs were constant over time within the measurement uncertainty which finally indicates that the equilibrium has been reached. In this work, the acquisition time of 300 ms per spectrum is sufficient for a good signal-to-noise ratio. With the established workflow, acquisition times up to several seconds from one single plug are possible.

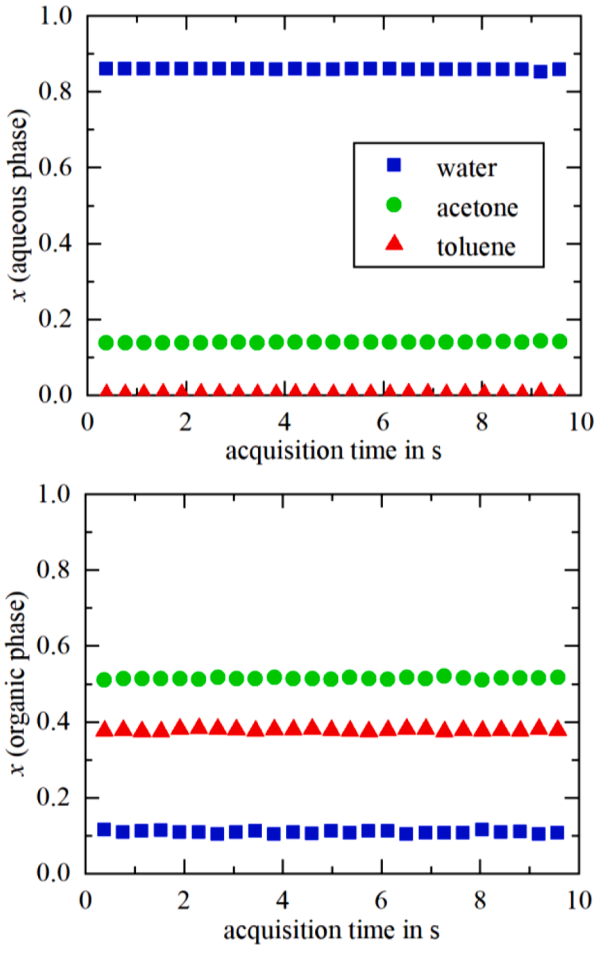

Fig. 6. Mole fractions in single plugs of organic and aqueous phase over time after start of the first acquisition (LLE 3 in table 2).

The measured equilibrium mole fractions are arithmetically averaged over all 25 measurements of single plugs. The calculated mean equilibrium mole fractions and the related mean absolute standard uncertainties for all components are presented in table 2.

Fig. 7 compared our data (given in table 2) and data measured by Friebel et al. at 22 °C in a triangular diagram [5]. Friebel *et al.* found that there is no significant temperature influence on the LLE for a temperature range of 20 °C to 30 °C [5]. Both, the measured equilibrium mole fractions which represent the binodale curve and the slope of the tie lines show excellent agreement within the uncertainties considering that Friebel *et al.* indicate a mean standard uncertainty of $u(x_i) = 0.008$ [5].

With the presented Raman setup, the measurement of the fully LLE (9 equilibrium concentrations) is possible within about 3 h, resulting in a sample consumption of less than 3 ml in total.

5. Conclusions and outlook

This work presents a promising measurement principle for the determination of liquid-liquid equilibria of water-organic systems in microfluidic plug flow. The small capillary dimensions and the inner circulations in the plugs result in fast equilibration of the phases. Using Raman spectroscopy, the precise concentration determination is rapid and in-situ. The automated workflow enables a strong reduction of the experimental effort and omits the error-prone manual sample preparation. For each tie line, an experimental time of 20 min is sufficient. The measurement of the complete miscibility gap, here consisting of nine tie lines, needed only about 3 h and less than 3 ml of chemicals in total.

Time-resolved single droplet tracking offers numerous further possibilities that will be part of future work. For example, the equilibration process or a reaction within a plug can be tracked and quantified.

Using this setup to investigate microfluidic plug flows and the setup presented in our previous work to investigate parallel microfluidic flows [7], we are now able to study a wide range of systems with versatile phase properties.

CRediT authorship contribution statement

Marvin Kasterke: Conceptualization, Methodology, Software, Investigation, Writing – original draft. **Julia Thien:** Conceptualization, Methodology, Formal analysis, Data curation, Writing – original draft. **Carsten Flake:** Software. **Thorsten Brands:** Conceptualization, Supervision. **Leo Bahr:** Supervision. **André Bardow:** Supervision, Writing –

Table 2
Liquid-liquid equilibrium mole fractions for the system acetone (x_1', x_1'') - toluene (x_2', x_2'') - water (x_3', x_3'') at $t = 25 \pm 0.2$ °C and $p = 1.013$ bar.

	x_1'	x_2'	x_1''	x_2''
LLE 1	0.5841	0.2066	0.2207	0.0041
LLE 2	0.5498	0.3041	0.1743	0.0028
LLE 3	0.5143	0.3776	0.1391	0.0021
LLE 4	0.4256	0.5064	0.0999	0.0013
LLE 5	0.3588	0.6007	0.0926	0.0010
LLE 6	0.2583	0.7300	0.0661	0.0001
LLE 7	0.2047	0.7875	0.0488	0.0010
LLE 8	0.1510	0.8448	0.0422	0.0015
LLE 9	0.0282	0.9710	0.0108	0.0000

Mean absolute standard uncertainties u are $u(x_1')$=0.0024, $u(x_2')$=0.0035, $u(x_3')$=0.0042, $u(x_1'')$=0.0006, $u(x_2'')$=0.0006 and $u(x_3'')$=0.0009.

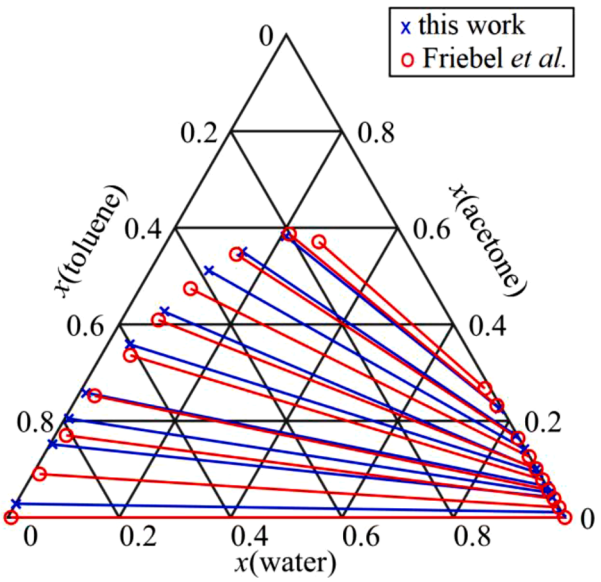

Fig. 7. Tie-lines of the acetone – toluene – water measured at $t = 25$ °C with the presented Raman setup and by Friebel et al. [5] at $t = 22$ °C.

review & editing. **Hans-Jürgen Koß:** Supervision, Writing – review & editing.

Declaration of Competing Interest

The authors declare the following financial interests/personal relationships which may be considered as potential competing interests:

Julia Thien reports financial support was provided by German Research Foundation.

Data Availability

Data will be made available on request.

Acknowledgement

This work was funded by the Deutsche Forschungsgemeinschaft (DFG, German Research Foundation) under Germany's Excellence Strategy – Exzellenzcluster 2186 "The Fuel Science Center".

Supplementary materials

Supplementary material associated with this article can be found, in the online version, at doi:10.1016/j.fluid.2022.113718.

References

[1] G.M. Kontogeorgis, R. Dohrn, I.G. Economou, J.-.C. de Hemptinne, A. ten Kate, S. Kuitunen, M. Mooijer, L.F. Žilnik, V. Vesovic, Industrial requirements for thermodynamic and transport properties: 2020, Ind Eng Chem Res 60 (13) (2021) 4987–5013. PMID: 33840887.

[2] R.D. Weir, T.W. de Loos, Measurement of the Thermodynamic Properties of Multiple Phases, Gulf Professional Publishing, 2005.

[3] D. Dechambre, C. Pauls, L. Greiner, K. Leonhard, A. Bardow, Towards automated characterisation of liquid–liquid equilibria, Fluid Phase Equilib 362 (2014) 328–334.

[4] B. Kuzmanović, M.L. van Delden, N.J.M. Kuipers, A.B. de Haan, Fully Automated Workstation for Liquid–Liquid Equilibrium Measurements, Journal of Chemical & Engineering Data 48 (5) (2003) 1237–1244.

[5] A. Friebel, A. Fröscher, K. Münnemann, E. von Harbou, H. Hasse, In situ measurement of liquid–liquid equilibria by medium field nuclear magnetic resonance, Fluid Phase Equilib 438 (2017) 44–52.

[6] M. Hübner, M. Minceva, Microfluidics approach for determination of the equilibrium phase composition in multicomponent biphasic liquid systems, Chemical Engineering Research and Design 184 (2022) 592–602.

[7] J. Thien, L. Reinpold, T. Brands, H.-.J. Koß, A. Bardow, Automated Physical Property Measurements from Calibration to Data Analysis: microfluidic Platform for Liquid–Liquid Equilibrium Using Raman Microspectroscopy, Journal of Chemical & Engineering Data 65 (2) (2020) 319–327.

[8] C. Xu, T. Xie, Review of Microfluidic Liquid–Liquid Extractors, Ind Eng Chem Res 56 (27) (2017) 7593–7622.

[9] M.N. Kashid, I. Gerlach, S. Goetz, J. Franzke, J.F. Acker, F. Platte, D.W. Agar, S. Turek, Internal Circulation within the Liquid Slugs of a Liquid–Liquid Slug-Flow Capillary Microreactor, Ind Eng Chem Res 44 (14) (2005) 5003–5010.

[10] N. Assmann, A. Ladosz, P. Rudolf von Rohr, Continuous Micro Liquid-Liquid Extraction, Chem Eng Technol 36 (6) (2013) 921–936.

[11] M.N. Kashid, A. Renken, L. Kiwi-Minsker, Gas–liquid and liquid–liquid mass transfer in microstructured reactors, Chem Eng Sci 66 (17) (2011) 3876–3897.

[12] S. Susanti, J.G.M. Winkelman, B. Schuur, H.J. Heeres, J. Yue, Lactic Acid Extraction and Mass Transfer Characteristics in Slug Flow Capillary Microreactors, Ind Eng Chem Res 55 (2016) 4691–4702.

[13] M. Alimuddin, D. Grant, D. Bulloch, N. Lee, M. Peacock, R. Dahl, Determination of log *D* via Automated Microfluidic Liquid–Liquid Extraction, J. Med. Chem. 51 (16) (2008) 5140–5142.

[14] J.G. Kralj, H.R. Sahoo, K.F. Jensen, Integrated continuous microfluidic liquid–liquid extraction, Lab Chip 7 (2007) 256–263.

[15] C.E. Poulsen, R.C.R. Wootton, A. Wolff, A.J. deMello, K.S. Elvira, A Microfluidic Platform for the Rapid Determination of Distribution Coefficients by Gravity-Assisted Droplet-Based Liquid–Liquid Extraction, Anal. Chem. 87 (12) (2015) 6265–6270.

[16] N.A. Marine, S.A. Klein, J.D. Posner, Partition Coefficient Measurements in Picoliter Drops Using a Segmented Flow Microfluidic Device, Anal. Chem. 81 (4) (2009) 1471–1476.

[17] P. Mary, V. Studer, P. Tabeling, Microfluidic Droplet-Based Liquid–Liquid Extraction, Anal. Chem. 80 (2008) 2680–2687.

[18] S.K. Luther, S. Will, A. Braeuer, Phase-specific Raman spectroscopy for fast segmented microfluidic flows, Lab Chip 14 (16) (2014) 2910–2913.

[19] G.L. Nelson, S.E. Asmussen, A.M. Lines, A.J. Casella, D.R. Bottenus, S.B. Clark, S. A. Bryan, Micro-raman technology to interrogate two-phase extraction on a microfluidic device, Anal. Chem. 90 (14) (2018) 8345–8353. PMID: 29733195.

[20] M.J. Pelletier, Quantitative analysis using raman spectrometry, Appl Spectrosc 57 (1) (2003) 20A–42A.

[21] T.C. Klima, A.S. Braeuer, Vapor-liquid-equilibria of fuel-nitrogen systems at engine-like conditions measured with raman spectroscopy in micro capillaries, Fuel 238 (2019) 312–319.

[22] C. Giraudet, K.D. Papavasileiou, M.H. Rausch, J. Chen, A. Kalantar, G.P. van der Laan, I.G. Economou, A.P. Fröba, Characterization of Water Solubility in *n*-Octacosane Using Raman Spectroscopy, The Journal of Physical Chemistry B 121 (47) (2017) 10665–10673.

[23] X.C. i Solvas, A. DeMello, Droplet microfluidics: recent developments and future applications, Chemical Communications 47 (7) (2011) 1936–1942.

[24] J. Scheffczyk, P. Schäfer, L. Fleitmann, J. Thien, C. Redepenning, K. Leonhard, W. Marquardt, A. Bardow, COSMO-CAMPD: a framework for integrated design of molecules and processes based on COSMO-RS, Molecular Systems Design & Engineering 3 (2018) 645–657.

[25] F. Alsmeyer, H.-.J. Koß, W. Marquardt, Indirect Spectral Hard Modeling for the Analysis of Reactive and Interacting Mixtures, Appl Spectrosc 58 (8) (2004) 975–985.

[26] P. Beumers, D. Engel, T. Brands, H.-.J. Koß, A. Bardow, Robust Analysis of Spectra With Strong Background Signals By First-Derivative Indirect Hard Modeling (FD-IHM), 172, Chemometrics and Intelligent Laboratory Systems, 2018, pp. 1–9.

[27] C. Peters, J. Thien, L. Wolff, H.-.J. Koß, A. Bardow, Quaternary Diffusion Coefficients in Liquids from Microfluidics and Raman Microspectroscopy: cyclohexane + Toluene + Acetone + Methanol, Journal of Chemical & Engineering Data 65 (3) (2020) 1273–1288.

[28] E. Kriesten, D. Mayer, F. Alsmeyer, C.B. Minnich, L. Greiner, W. Marquardt, Identification of Unknown Pure Component Spectra By Indirect Hard Modeling, 93, Chemometrics and Intelligent Laboratory Systems, 2008, pp. 108–119.